

Zarillo, G. A., and Brehin, F. G. A. 2007. Hydrodynamic and Morphologic Modeling at Sebastian Inlet, FL. *Proceedings Coastal Sediments '07 Conference*, ASCE Press, Reston, VA, 1297-1310.

## HYDRODYNAMIC AND MORPHOLOGIC MODELING AT SEBASTIAN INLET, FL

Gary A. Zarillo<sup>1</sup> and Florian G. A. Brehin<sup>2</sup>

1. Department of Marine and Environmental Systems 150 West University Blvd.  
Florida Institute of Technology Melbourne, FL 32901

[zarillo@fit.edu](mailto:zarillo@fit.edu)

2. Department of Marine and Environmental Systems 150 West University Blvd.  
Florida Institute of Technology Melbourne, FL 32901

[fbrehin@fit.edu](mailto:fbrehin@fit.edu)

**Abstract:** Numerical model simulations of tidal inlet hydrodynamics, sand transport and topographic change were performed using the Coastal Modeling System (CMS) to investigate the morphological response to time varying forcing, sediment texture, and the influence of rock reef outcrops within the Sebastian Inlet system. The presence or absence of rock within the inlet throat and in the surf zone on the south side of the inlet resulted in distinctive differences in topographic changes to the ebb shoal over a year long simulation. Comparisons between three sand transport formulations over a shorter period (2 months) showed some variation among the formulations, but predicted net topographic changes were well within an order of magnitude. Comparisons between predicted and measured net topographic changes demonstrated agreement in terms of pattern. Agreement in absolute terms improved as the model spatial resolution was refined by decreasing cell sizes.

### INTRODUCTION

Inlet/bay systems and their morphologic features exist in dynamic equilibrium, with sand fluxes between shoal sand reservoirs due to complex interactions with the surrounding forcing mechanisms. The accurate modeling of the morphologic evolution of tidal inlet shoals is an important management tool, since they control sediment budgets. Inlet hydrodynamics depend on physical forcing, inlet and bay geometry, bottom topography, and presence of stabilizing structures that influence

sedimentation and flow patterns. Controlling jetties have been constructed at most of the smaller tidal inlet systems of the U.S East and Gulf Coasts to prevent shoaling and safety of navigation channels and stabilize the inlet location. Stabilization may also influence inlet evolution by enhancing the formation of ebb shoal and flood shoal deposits. Net longshore sediment transport and wave forces reshape the ebb shoal through a mechanism in which sediment is bypassed around the inlet, forming a bypass bar and eventually an attachment bar which connects the ebb shoal to the downdrift beach. As the shoal system of a stabilized inlet evolves, variations within the wave climate can abruptly increase or decrease the volume of sediment on the ebb or flood shoals and cause temporary, but large variations in the volume of sand bypassing the inlet (Zarillo et al., 2003).

Regional sand management has become a national issue that requires data collection and monitoring of tidal inlets and surrounding beaches as well as better predictive tools for predicting morphology changes. Computationally efficient numerical models to reproduce and predict sedimentation patterns at inlets such as ebb-shoal growth, scour patterns around structures, cross shore transport between shoals have been developed under the Coastal Inlets Research Program (CIRP) at the Coastal and Hydraulics Laboratory of the U.S. Army Water Ways Experiment Station. Termed the Coastal Modeling System (CMS) the suite of models provides realistic simulations of inlet behavior. However, the remaining limitations of numerical modeling include the computation times, which increase with spatial resolution, limited morphologic constraints to prevent over prediction of topographic change, and the lack of extensive field data to calibrate model results. The model application presented in this paper summarizes the results based on the state of the CMS technology as of the middle of 2006.

## **OVERVIEW OF THE MODELING APPROACH**

The CMS is based on the M2D model, which is a time-dependant, 2-D finite difference circulation and morphology model, which calculates water surface elevations, two components of the current and sediment transport on a rectilinear grid (Militello et al., 2004). Coupling of M2D with the Steady Spectral wave model STWAVE (Smith et al, 2001) was performed through the Surface Modeling System interface (SMS) using the steering process to include the radiation stresses and wave induced currents (Zundel, 2000).

The CMS includes three sediment transport modules: Watanabe formulation (Watanabe. 1987), the Lund-CIRP formulation, and Advection-Diffusion (AD) enhancement of the Lund Formulation ((Buttolph et. al, 2006). The sediment transport formulations are directly coupled to the M2D model along with a continuity-based calculation of morphologic change that considers sediment volume exchanges among computational cells (Buttolph et al., 2006). The Watanabe formulation for total load is a function of an empirical coefficient for wave irregularity, bed shear stress, critical shear stress of incipient motion, the water density, gravitational acceleration and total depth averaged current velocity. The Lund-CIRP formulation is more complex including the added the benefits of writing out bed load and total transport as separate values and calculating the wave energy

dissipation. In the AD formulation diffusivity terms in the horizontal dimensions are added to enhance sediment motion. Another important feature included in the model calculations is the representation of non-erodible cells (Hanson and Militello, 2005) that can be used to represent shore protection structures including breakwaters and jetties, as well as natural features.

### **MODEL APPLICATION AT SEBASTIAN INLET, FL**

This paper presents several examples from an ongoing modeling effort at Sebastian Inlet, FL to investigate the sediment transport and morphological evolution. Numerical simulations of the coupled circulation/wave models (M2D/STWAVE) are discussed under the following topics: 1. preliminary hydrodynamic runs and calibration, 2. hard bottom subroutine testing, 3. shorter term (2 months) model test cases run applying different sediment transport formulations. Computed topographic changes were analyzed and compared with measured data from bathymetric surveys.

Sebastian Inlet is located in the southern part of the Indian River Lagoon (IRL) on the east coast of Central Florida. Rock outcrops of coquina line the bottom of the inlet throat and form a rock reef area exposed in the surf zone on the southern side of the inlet. The inlet is also characterized by a small throat cross section area and a large bay (IRL), which promotes strong currents through the. The present Sebastian Inlet was artificially cut into the coquina of the Late Pleistocene Anastasia Formation in the late 1940's and stabilized by offset jetties from 1950's to 1970's. The present configuration of the inlet (Figure 1a & 1b.) includes a 250 meter-long curved north jetty and a shorter straight south jetty of approximately 75 meters.

The main morphologic features include the ebb shoal and bypass bar, which is obliquely oriented to the southern beaches and connects to the attachment bar about 700 m south of the inlet entrance, a large flood shoal, and an excavated sand trap (Figures 1a & 1b). The mean tidal range is approximately 1 meter. The east central Florida wave climate is moderate having a mean annual wave height of 0.6 meter (Zarillo *et al.*, 2003). However the wave regime is subject to strong seasonal variations in energy and approach, punctuated by the higher wave energy from northeasters and tropical storms and hurricanes. Analysis of the 15 years of surveys of the inlet indicates that the inlet is in state of quasi-equilibrium in terms of shoal volumes, but the dynamic ebb shoal can gain or lose more than 100,000 m<sup>3</sup> of volume in a single year and controls the inlet sediment budget. The net sand budget of about 120,000 to 230,000 cubic m<sup>3</sup>/yr is thought to be driven by a few extratropical storms creating southerly drift, whereas tropical systems from the south tend to drive longshore sediment transport toward the north (Zarillo *et al.*, 2003). Figure 2 summarizes the wave climate in terms of the longshore component of wave power. The cumulative plot indicated that the net component is directed south but that reversals and strong variations in magnitude are common.

### **Model Setup**

In the Sebastian Inlet region the model grid was setup on the inner continental shelf and shoreface from approximately 12 km north of the Inlet to 12 km south of the inlet (Figure 2). Data sets for model grid development and model boundaries include

topographic data, wave data from the Wave Information System (WIS) and from local monitoring programs, water level data, and sedimentologic data available from local sand source investigations, and beach condition surveys.

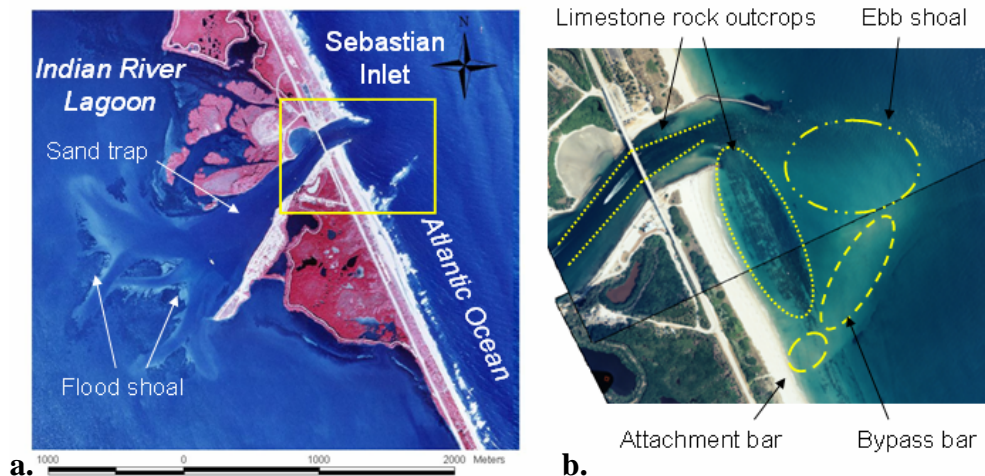


Figure 1. Study area. Note the waves breaking around the southern bypass bar. Hard bottom appears as dark bands on the aerial image.

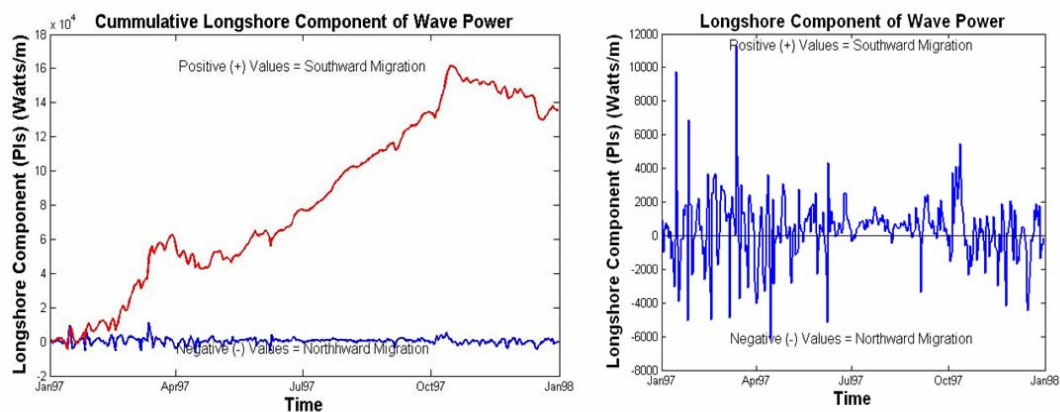


Figure 2. (a) Cumulative Longshore component of wave power, (b) longshore component of wave power.

Topographic data from the National Geodetic Data Center (NGDC) was combined with shoreface data from 1997. The simulation was forced by three measured water surface elevation (WSE) time series applied at the north lagoon, south lagoon, and ocean boundaries of the model grid. Wave inputs into STWAVE consisted of 365

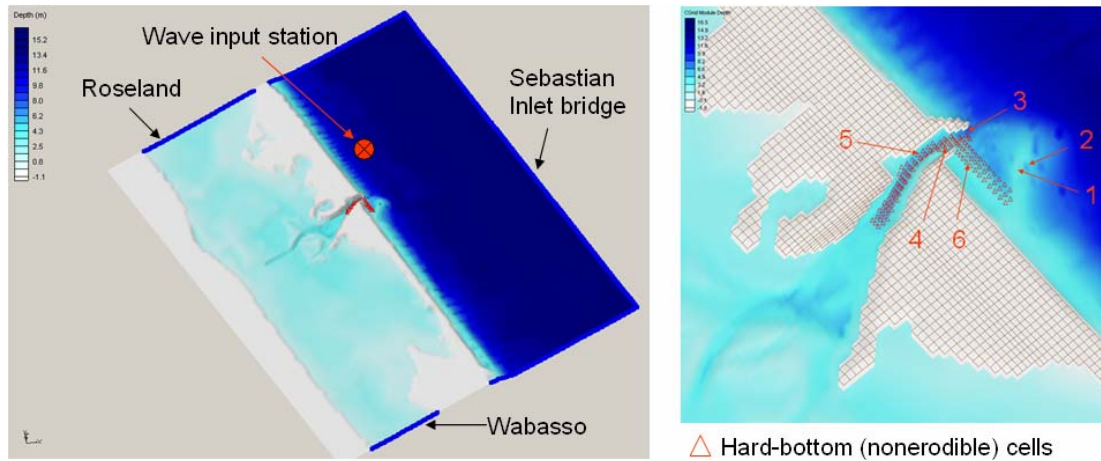


Figure 3. M2D grid and water surface elevation boundaries. The bottom topography contours are in meters.

directional spectra for coupling to M2D through a steering module that updated the wave field every 24 hours. Hind cast wave data from a nearby WIS station were propagated within a regional STWAVE grid to obtain the nearshore wave climate. The wave climate during the simulation time mainly consists of fair weather conditions with some storm events in summer and more frequent storms in fall and winter months. The largest wave heights were approximately 2 meters along with periods ranging from 4 to 15 s. The M2D grid cells corresponding to rock outcrops were selected and tagged as non-erodible (Figure 3). The depth of maximum erosion was set to 20 cm to account for occasional sand layers on the hard substrate. Observation cells were selected at different points of the model domain to extract time series of model outputs for analysis. For the longer term model runs (12 months) and testing the hard bottom routine, the circulation and wave model resolution was set to 50 meters. The two model cases used the Watanabe transport formula, sediment grain size set at 0.2 mm, the Watanabe sediment transport coefficient A set to 0.5, and total simulation time set to one year (8760 hours). For the three model cases comparing sand transport formulations and topographic changes between formulations the offshore cell sizes were set to 50 meters and refined to 25 meters in the inlet vicinity. Sediment grain size was set to 0.2 mm and simulation time was set to 1344 hrs (56 days).

### Calibration and Preliminary Hydrodynamic Runs

A first step prior to sediment transport computations consisted of calibrating the hydrodynamic model. Predicted time series of water surface elevations were compared with measured elevations in terms of amplitude and phase. No measured current data were available for the model period. A comparison between computed and measured water surface elevations for Wabasso, FL tide station near the south boundary of the model is shown in Figure 4. Computed and measured elevations were found to match closely in terms of amplitude and phase. An example of computed current magnitude and direction during the ebb stage is displayed in Figure 5. Average computed velocities ranged from near zero behind the flood shoal to around 2 m/s between the two jetties confining the inlet throat. Stronger currents were found



in the inlet channel and throat. The model represents the ebb jet feature in between the jetties, where tidal currents peak and eddies forming on both sides and propagate offshore as current decreases around the ebb shoal. Current velocity was found to be strongly attenuated by the shoals.

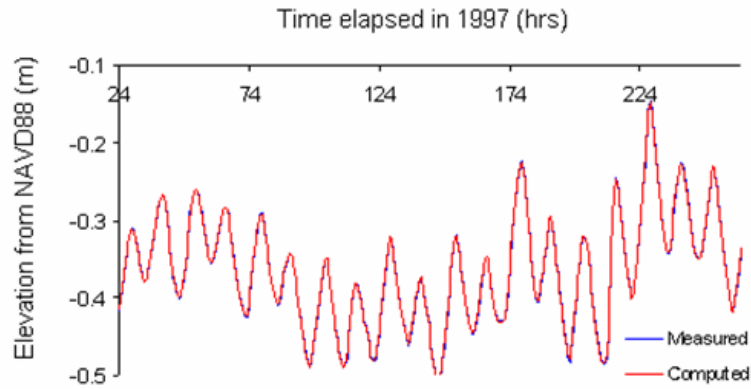


Figure 4. Model calibration: measured versus computed water surface elevations at Wabasso, FL.

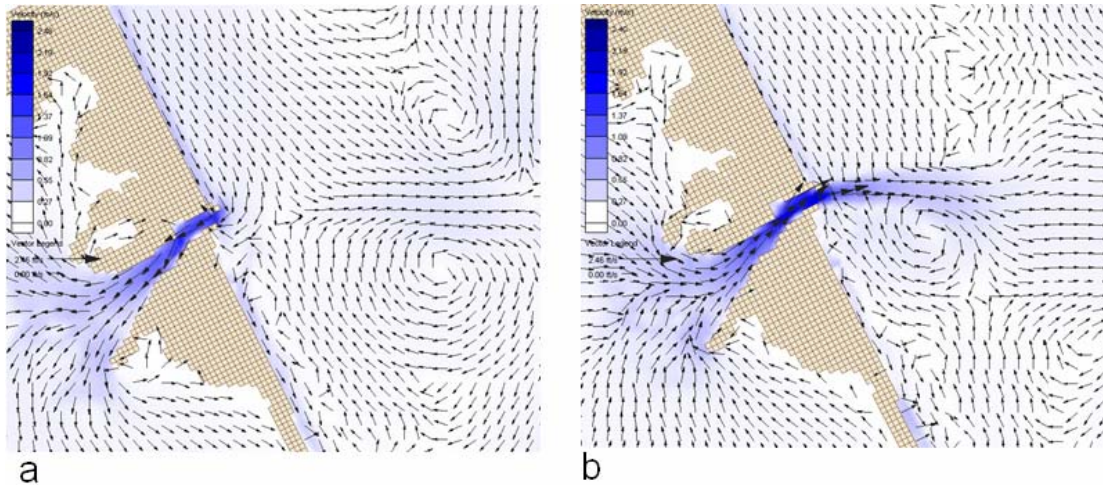


Figure 5. Current magnitude and directions extracted during a) flood stage and b) ebb stage.

During tests of the wave model wave height and direction were extracted for two cases: a northeaster and storm waves approaching from the south (Figure 6). Shoaling over the crest of the ebb shoal and along the bypass bar increased wave heights followed by a decrease and breaking at the shoreline. Strong wave refraction occurred around the ebb shoal/bypass bar area, especially when waves approached from the North East. Wave penetration into the inlet throat was predicted when waves were coming from the South East.

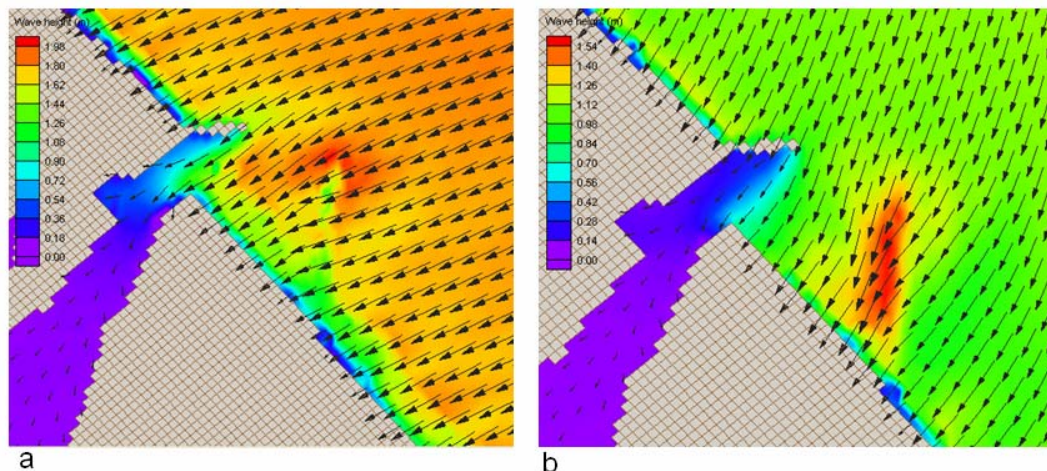


Figure 6. Predicted wave height and direction for a) swell approaching from the south typical of tropical systems b) Extratropical northeaster storm.

### Long Term Runs

Model test cases were run with and without selected model cells tagged as non-erodible to simulate the influence of rock outcrops on inlet dynamics. Computed net topographic change after a one year simulation under the Watanabe sand transport formulation is shown in Figure 7. Erosion areas corresponding to negative values are represented by blue colors and deposition areas (positive values) are represented by red colors. In the two model cases, channel bank erosion was observed, as well as scour at the seaward end of the offset jetties corresponding to areas of maximum current velocities during ebb and flood stages. Patches of erosion alternating with accretion were predicted on north and south shoreface areas, as well as over the flood shoal. For the south beaches and attachment bar, more complex patterns with patches of accretion and erosion alternating on the upper shore-face, probably due to interactions with rock reef.

Transient and permanent sand deposition is also predicted within the inlet throat section and ebb shoal complex and in both cases, a substantial net growth of the ebb shoal is predicted. When model cells were tagged as non-erodible through main inlet conveyance channel bank erosion increased as the inlet adjusted to a larger equilibrium cross-sectional area and the terminus of the ebb shoal extended farther from the inlet throat. Cross-shore transport on the bypass bar was observed for both runs, but deposition and erosion areas were reversed.

The hard bottom influence at specific cells corresponding to rock reef outcrops was investigated by extracting time series of topographic changes at high temporal resolution (Figure 8). Observation points 1, 2 and 3 were cells tagged as non-erodible with an initial layer of sand of 20 cm. At point 1, located on the reef in the outer surf-

zone of the south beaches, slight erosion of about 5 cm was predicted in the run, whereas net erosion to a depth of 0.5 meters was predicted in the run without non-erodible cells. At observation point 2 on the south side of the inlet throat episodic scour and deposition was predicted along with net erosion after about six months. The hard bottom run shows a less variable pattern of scour and deposition but with maximum erosion limited to 20 cm. Point 3 in a channel margin area west of the inlet throat experienced episodic scour and deposition without hard bottom and deposition when tagged as a hard bottom cell.

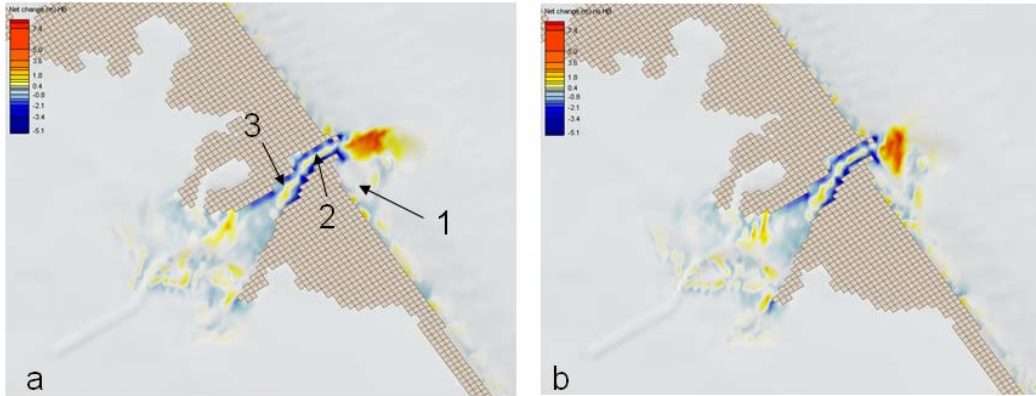


Figure 7. Computed Net topographic change after 1 year run under Watanabe formulation a) hard bottom and b) no hard bottom. Numbers correspond to observation cells for time series extraction.

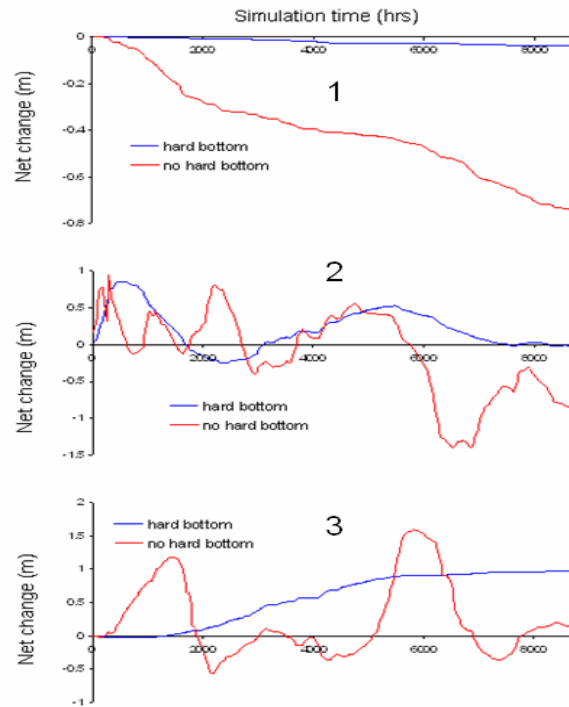


Figure 8. Extracted time series at observation stations for 1 year run (1997) under Watanabe formulation hard bottom versus no hard bottom.



### Comparisons Between Sand Transport Formulations

Computed net topographic change after two months of simulation (1344 hours) is compared for the runs applying the Lund-CIRP formulation (Figure 9), Watanabe (Figure 10), and Advection Diffusion formulation (Figure 11). For all runs, the greatest erosion occurred along the margins of the inlet channel, whereas deposition is observed in the inlet channel. The Advection-Diffusion formulation showed more complex patterns, with less sand deposition in the channel, more deposition on the shoreface. All formulations agree in terms of sedimentation pattern including sand transport over the bypass bar with erosion on the outer part and deposition on the inner bar. However, the AD formula is the only one to reproduce natural bypassing and patches of sand accumulation on the attachment bar and shore-face between the south jetty and attachment bar. Under the Lund formulation, a small amount of sand was bypassed, but erosion was the dominant pattern between the beach and the first reef line. Over the flood shoal calculated net topographic changes very are small and mostly concentrated on the margin of the sand trap consistent with reality. Similar to the ocean side of the inlet patchy sand deposition is predicted by the AD calculations.

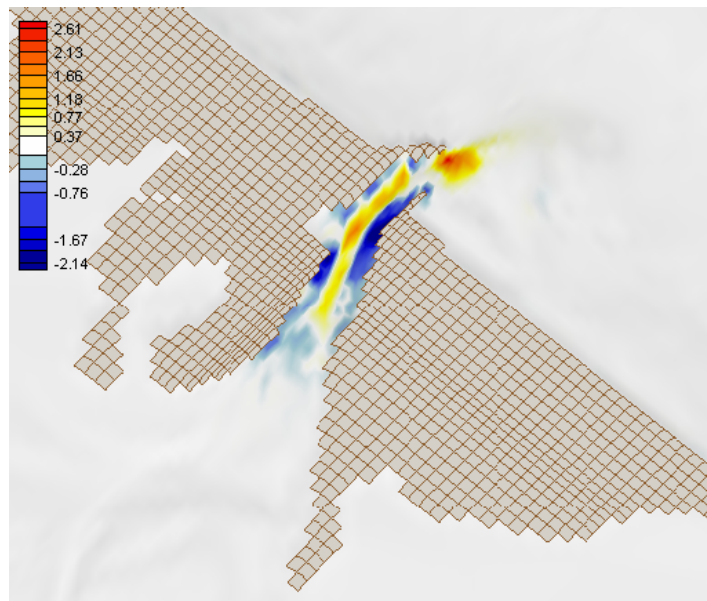


Figure 9. Computed net topographic change after 2 months of simulation under Lund-CIRP formulation.

Time series of bottom topography extracted at five observation cells shown in Figure 3 were used to compare the net predicted bottom change from each formulation. The sedimentation time series shown in Figure 12 agree well with visual observations of net change including erosion on the outer part of the bypass bar (point 2) and

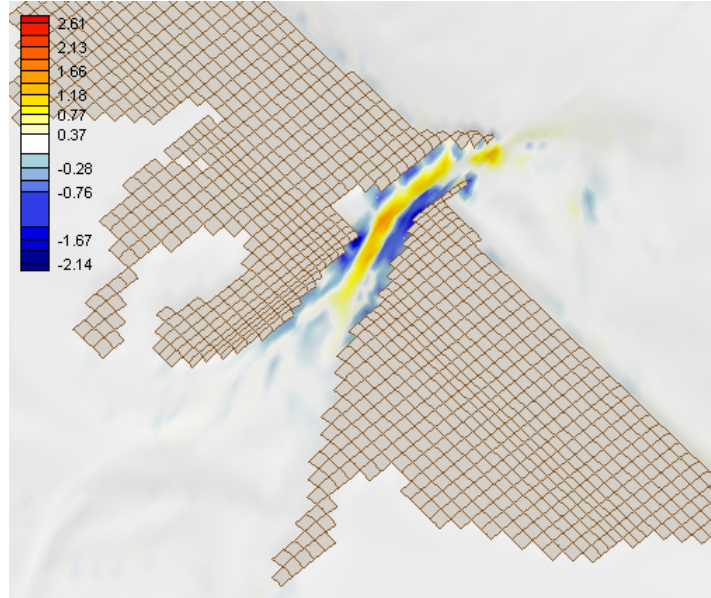


Figure 10. Computed net topographic change after 2 months of simulation under Watanabe formulation.

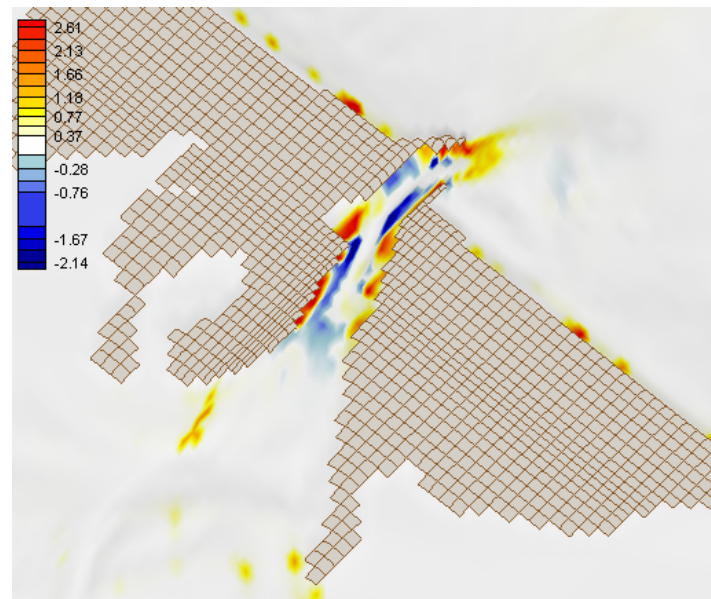


Figure 11. Computed net topographic change after 2 months of simulation under Advection-Diffusion formulation.

accretion on the inner part (point 1). For the three formulations, the overall trend is in accretion. Under Lund and AD formulas, the same trends of scour and deposition were observed, with the main difference in the magnitude of the net change. Computed net erosion at observation cell 2 was predicted by the three formulas. However, the magnitude of the net topographic change under the Watanabe formula was smaller compared to Lund and AD. Observation cell 3 is located off the east tip

of the North jetty. Here accretion was predicted by the three sediment transport formulas. Under the AD formula the predicted time series was more variable, whereas Lund and Watanabe formulas produced a more linear increase in net topographic change. Observation cell 4, 5, and 6 (Figure 2) were tagged as hardbottom cells. At cell 4 located off the tip of the south jetty, between the inlet channel and jetty structure the largest deposition was observed under the AD formula. Results diverge by the end of the run when scour was predicted by Lund. Model results at observation cell 5 on the North Channel margin of the inlet throat are similar for about half the simulation. However during the second half net deposition at this hardbottom cell under the AD formulation decreased while the other formulations continued to predicted a net increase. Model results at cell 6 is located on the rock reef outcrops located on the shoreface south of the inlet entrance indicated near zero net change under all three formulations. Only the AD results showed episodes of slight deposition and erosion.

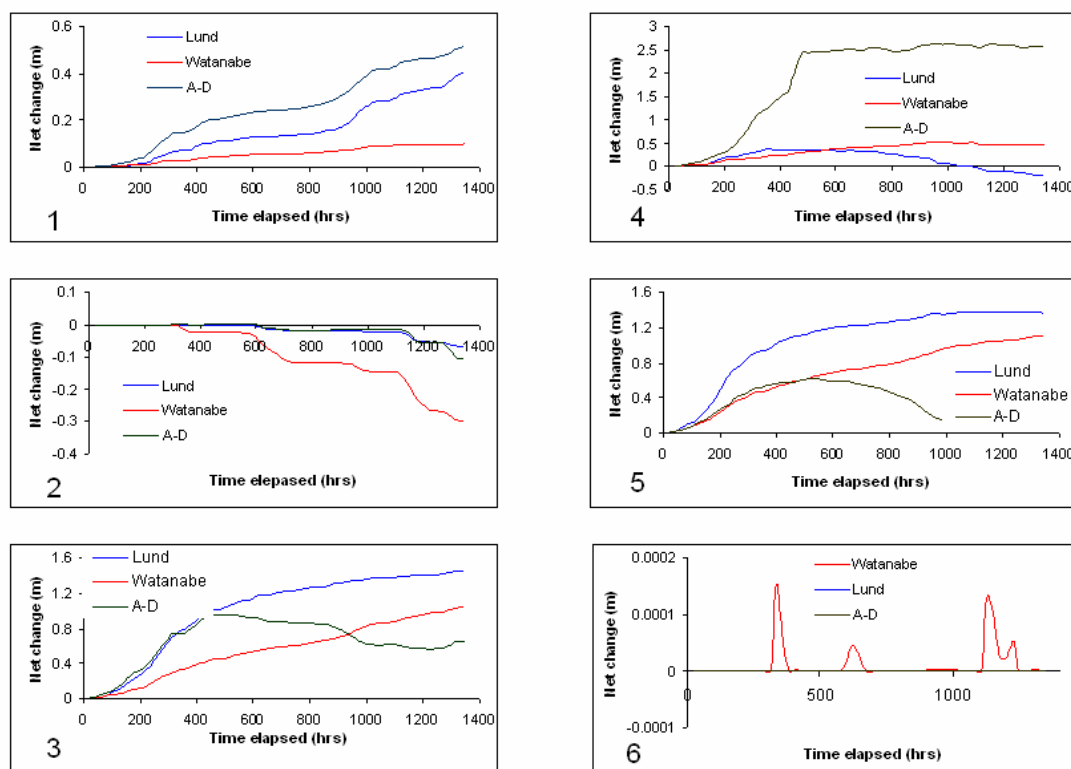


Figure 12. Time series of net bottom change extracted at each observation point.

## SUMMARY AND DISCUSSION

Computed tidal currents were well within the range of magnitude determined by field measurements. The circulation model reproduced the expected ebb-jet during ebb stage, as well as the expanding turbulent wake. Through the longer term model runs wave driven currents were predicted on the upper-shoreface cells to the north and south of the inlet entrance, whereas tidal currents controlled sand transport within the inlet entrance. Predictions from the wave model reproduced complex wave refraction

and breaking over the ebb shoal and bypass that influence local sand transport directionality. During extratropical storms wave driven circulation patterns induced northward sand transport on the south side of the inlet between the south jetty and the attachment bar.

The largest computed net topographic changes were related to the hydrodynamic regime within the inlet/bay system. Channel bank erosion occurred, as well as scour at the seaward end of the offset jetties corresponding to areas of maximum current velocities during ebb and flood stages. Transient and permanent sand deposition was predicted within the inlet throat section and ebb shoal complex. The presence or absence of rock within the inlet throat and in the surfzone on the south side of the inlet resulted in distinctive differences in topographic changes to the ebb shoal over a year of real time simulation. When model cells were tagged as non-erodible through main inlet conveyance channel, bank erosion increased as the inlet adjusted to a larger equilibrium cross-sectional area. Episodic scour and deposition patterns across the shoreface were associated with storm conditions frequency and intensity and reversal in longshore transport.

Comparisons between sand transport equations showed some variation among the formulations but net topographic changes predicted from the formulations were well within an order of magnitude. However, the AD formula was the only one to reproduce bypassing and sand accumulation on the attachment bar. Under the Advection-Diffusion formulation, more complex sedimentation patterns were predicted. Less deposition occurred in the channel, which may be due to increased quantity of sediment in suspension in the channel.

Comparisons between predicted and measured topographic changes on an annual basis qualitatively agreed in terms of morphological evolution pattern. Agreement in absolute terms improved as the model spatial resolution was refined by decreasing cell sizes. Figure 13 is a comparison between predicted and modeled topographic changes at the entrance of Sebastian Inlet between March and September of 1997. The model predicted erosion and deposition patterns observed over the ebb shoal and bypass bar area and erosion along the south jetty. However, predicted deposition in a topographically low area off the end of the north jetty was not present in the survey data. Some of this difference could be due to inadequate representation of the north jetty and may require better resolution and further tuning of sand transport calculations. In addition, the sand transport module considered uniform grain sizes over the entire inlet. Material is usually coarser in areas of intense hydrodynamics, such as around the jetty fillets and on the ebb shoal. A more recent version of the M2D model now allows a variable grain size to be specified over the model grid.

## **CONCLUSIONS**

Numerical simulations of coupled circulation, wave and sediment transport models were applied to Sebastian Inlet to calculate the morphology change and determine the influence of limestone rock outcrops on inlet dynamics. Evolution of morphology at Sebastian Inlet was found to be associated with the ebb-jet and wave-induced transport. General patterns of ebb shoal growth, sand bypassing, and scour of the

channel banks and around the jetties were reproduced by the CMS-M2D. The hard-bottom feature of the M2D model was effective in reducing the sediment transport in the channel and on the shoreface to the south of the inlet where natural rock reef outcrops occur. The inclusion of hardbottom cells though the main inlet channel induced erosion of the channel banks as the inlet adjusted to a larger equilibrium cross-sectional area. Adjustments to the ebb shoal topography in the model simulations was controlled by interactions between tidal and wave forces. Specifying non-erodible cells along model inlet channel produced deposition over the seaward portions of the ebb shoal most likely as a result of decreased sediment impoundment and increased regions of channel margin areas. Known patterns of topographic change on the shoreface were reproduced by the model cases, with erosion on the outer part and deposition on the inner part of the bypass bar. Predicted and measured topographic changes at Sebastian Inlet qualitatively agree. Further tuning and refinement of sand transport calculations are required to improve the match between model and real topography.

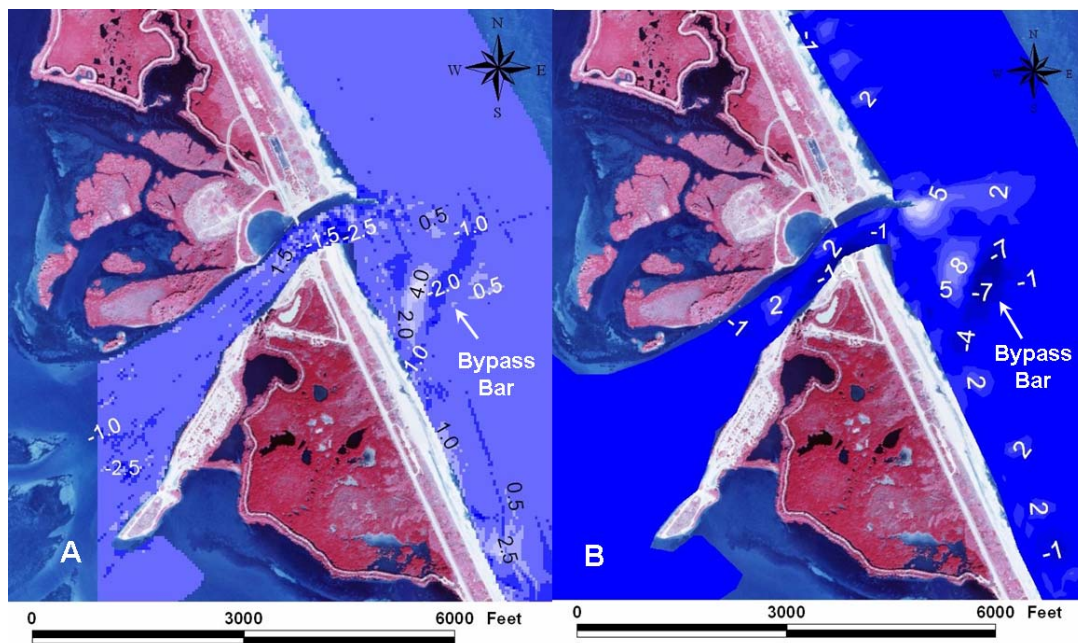


Figure 12. Comparison between predicted (A) modeled (B) topographic changes between March and September of 1997. Values of topographic change are in feet.

#### ACKNOWLEDGEMENTS

The U. S. Army Corps of Engineers (USACE) Coastal Inlets Research Program (CIRP) provided support for this research. The Sebastian Inlet Tax District kindly provided survey data and hind cast directional wave data. The St. Johns River Water Management District provided water level time series used to drive model



## REFERENCES

- Buttolph, A. M., Reed, C. W., Kraus, N. C., Ono, N., Larson, M., Camenen, B., Hanson, H., Wamsley, T., and Zundel, A. K. (2006). "Two-Dimensional Depth-Averaged Circulation Model CMS-M2D: Version 3.0, Report 2, Sediment Transport and Morphology Change," ERDC/CHL TR-06-09, U.S. Army Engineer Research and Development Center, Vicksburg, MS.
- Dombrowski, M. R., 1993, "Inlet and Management Practices: Southeast Coast of Florida", *Journal of Coastal Research Special Issue n. 18*, pp. 29-57.
- Hanson, H. and Militello, A., 2005, "Representation of non-erodible (hard) bottom in two-dimensional morphology change models", *Coastal and Hydraulic Engineering Technical Note ERDC/CHL CHETN-IV-63*, U.S. Army Engineer Research and Development Center, Vicksburg, MS.
- Hoeke, R.K., 2001. Decadal time scale where morphodynamics determined from remotely sensed shoreline positions. *Master's Theses, Division of Marine and Environmental Systems, Florida Tech*, Melbourne, FL.
- Lin, L., Kraus, N. C., and Barcak, R. G., 2003. "Modeling Coastal Sediment Transport at the Mouth of the Colorado River, Texas", *Estuarine and Coastal Modeling, 8<sup>th</sup> International Conference on Estuarine and Coastal Modeling* Malcolm L. Spaulding - Editor, November 3–5, 2003, Monterey, California, USA.
- Militello, A., C.W. Reed, A.K. Zundel, and N.C. Kraus. 2004. Two-Dimensional Depth-Averaged Circulation Model M2D: Version 2.0, Report 1: Technical Documentation and User's Guide, ERDC/CHL TR-04-02, Vicksburg, MS: U.S. Army Engineer Waterways Experiment Station.
- Smith, J. M., A.R. Sherlock, D.T. Resio. 2001. STWAVE: Steady-State Spectral Wave Model User's Manual for STWAVE, Version 3.0. TR-01-1 Vicksburg, MS: U.S. Army Engineer Waterways Experiment Station.
- Zarillo, G. A., Kraus, N. C., and Hoeke, R. K., 2003, "Morphologic Analysis of Sebastian Inlet, Florida: Enhancements to the Tidal Inlet Reservoir Model", *Proceedings Coastal Sediments '03*.
- Zundel, A. K., 2000, "Surface water modeling system reference manual", Brigham Young University, Environmental Modeling Research Laboratory, Provo, UT.